Hydrate Dissociation Rates in Pipelines[1]

S.K. Kelkar[2], M.S. Selim[3], E.D. Sloan[2,4]

1. Paper presented at the Thirteenth Symposium on Thermophysical Properties, June 22-27, 1997, Boulder, Colorado, U.S.A.

2. Center for Hydrate Research, Colorado School of Mines, Golden CO-80401

3. Dept. of Chemical Engineering, Colorado School of Mines, Golden, CO-80401

4. To whom correspondence should be addressed

ABSTRACT

Recent laboratory and field data suggest that hydrates form very porous pipeline plugs which transmit pressure freely, while hydrates act as significant flow obstructions. The blocked flow causes an ocean pipeline to rapidly equilibrate to the ocean temperature at 4°C. When the hydrate plug is dissociated through total depressurization of the pipeline, the hydrate plug will convert to an ice plug which requires significantly longer to dissociate than the hydrate. This work indicates that there is an optimum pipeline pressure for the most rapid dissociation of all solid phases resulting from hydrate pipeline blockages. Surprisingly, the high ice thermal diffusivity and a high thermal gradient provides the highest heat flux when some ice is present.

Keywords: hydrate, ice, ocean, pipeline, optimum, depressurization.

1. INTRODUCTION

Natural gas hydrates are crystals with well-defined structures (1) which occur when water encages molecules smaller than 1.0 nm at low temperatures and elevated pressures. Since virtually all production of natural gases involves free water, pipeline hydrate crystals can grow to a size which jeopardizes fluid flow. To prevent pipeline flow blockages, annually about $0.5 billion (US) in chemicals are injected as thermodynamic inhibitors (e.g. methanol or glycol, (2)) or more recently kinetic inhibitors (e.g. n-poly(vinyl caprolactam) (3)).

However, over the life of a pipeline hydrate inhibition injection may be interrupted due to pump failure, chemical supply line fracture, etc., resulting in pipeline blockage which may require days or weeks to clear. Blockage of normal pipeline flows also prevents the flow of methanol from reaching the hydrate plug site. Dissociation through heating is limited because the plug location and extent are not well-defined, and heating lengthy subsea pipelines is costly.

Usually some combination of the above techniques is used together with the principal technique for hydrate plug remediation, namely depressurization. When only one end of a hydrate plug is depressurized, two unwanted results may occur: 1) Joule-Thomson cooling may occur for very porous hydrate plugs which may result in the plug downstream forming more hydrate (4,5), or 2) if the hydrate plug releases at the pipeline wall, the upstream pressure causes a pipeline projectile, sometimes with disastrous safety results at pipeline bends, elbows, etc. (6).

When a plug occurs at a deep-sea pipeline, the situation is particularly delicate, as illustrated in Figure 1. To the left of the three phase (L_W-H-V or I-L_W-V) lines hydrates or ice can form, while to the right only fluids can exist. Because the lowest ocean temperature is 4°C, ice formation is not a normal operating concern, although ice could block flow effectively. When hydrates form, flow is blocked so that the plug temperature rapidly decreases to the ocean floor temperature of 4°C (39.2^{o}F) at the pipeline pressure. Figure 1 is a schematic of a pipeline hydrate plug at point A in the two-phase (H-V) region, where any liquid water has been converted to hydrate.

Pressure reduction is accompanied by a temperature decrease at the hydrate interface. If the pipeline is rapidly depressurized, either Joule-Thomson (isenthalpic) cooling (line AD) or isentropic cooling (line AE) at the hydrate may worsen the problem. If the pressure is reduced extremely slowly, isothermal depressurization (line AC) results. Usually an intermediate pressure reduction rate causes the hydrate interface temperature to be significantly less than 4°C, so that heat influx from the pipeline wall causes solid melting.

With rapid or extreme pressure reduction (e.g. to atmospheric pressure) the hydrate temperature will decrease below 0°C, so that water from dissociated hydrate will rapidly convert to ice below the solid-liquidus (I-L_W-H) shown in Figure 1. If ice formation occurs with hydrate dissociation, then the question arises, "How will ice dissociation rates compare to hydrate dissociation rates in an ocean pipeline?" The object of this work was to determine if there is an optimum method for hydrate depressurization, through simple modeling techniques.

2. MATHEMATICAL MODEL

Previously we modeled hydrate dissociation as a non-porous moving boundary plug (7) in which depressurization from both ends resulted in dissociation progressing from the ends toward the middle. Recently however, laboratory (6) data suggest that hydrates are very porous, (from 33 to 84% porosity). In a field study (9) hydrate plugs were intentionally formed and removed from a North Sea line in the Tommeliten Gamma field; these plugs were also found to be very porous. Such results have prompted others (8) to model hydrate dissociation using Darcy's law, a steady-state equation for flow, inserted into a non-steady state equation for pressure change.

As an alternative, consider hydrates with a porosity of 50% or more, which may transmit pressure very well while still acting to prevent free flow of gas. With highly porous hydrates, depressurization will result in a uniform hydrate dissociation temperature in equilibrium with the pressure.

In this model for highly porous hydrates, the hydrate dissociation temperature is uniform throughout the plug, as determined by a step-reduction of the pipeline pressure on each side of the plug. After depressurization negligible pressure drop occurs either radially or longitudinally along the pipe or the plug. In addition, radial hydrate dissociation is considered because the radial dimension (less than 1m) may be substantially less than the length of a hydrate plug (typically 10m) in a pipeline.

A schematic of our hydrate dissociation model is presented in Figure 2. Figure 2a shows an inner hydrate core (A) surrounded by an ice layer (B), which is enclosed in a water layer (C) adjacent to the pipe wall (D). Figure 2b shows the temperature profile from 4°C at the pipe wall, to 0°C at the water-ice interface, to the hydrate dissociation temperature at the ice-hydrate interface, where it remains uniform throughout the hydrate layer. As a result, there are two two-phase boundaries, one at the water-ice boundary (X_1) and a second (X_2) at the ice-hydrate boundary. We are particularly interested in the rate of progress of X_1, which determines the disappearance of the final solid (ice), since any solid phase constitutes a flow obstruction in a pipeline.

Two additional simplifications were made: (1) the pipeline curvature is neglected so that we deal with one-dimensional rectangular coordinates, and (2) we assume that the pressure is step changed to a low value on both sides of the plug, so that the hydrate temperature is uniform at the dissociation value of the depressurization.

This work simulates the case of pipeline depressurization when the plug is formed between a platform and the pipeline shore landing, so depressurization on both sides of a plug can be achieved. This work does not address single-sided depressurization, as may occur for hydrate plugs between the ocean well-head and an offshore platform.

2.1. EQUATIONS, BOUNDARY CONDITIONS, AND RESULTS

The assumptions in the model are as follows:

1. Hydrates are highly porous and transmit the pressure equally throughout the hydrate,
2. At initial time the hydrate pressure will be step-reduced to the desired pressure,
3. The hydrate dissociation temperature will be set by the applied pressure,
4. Dissociation temperature of hydrates is the same everywhere,

5. Only radial dissociation is considered, and
6. Curvature is neglected so that rectangular coordinates may be used.

2.1.a. At T_D< 273K While Three Phases (Hydrate-Ice-Water) Are Present.

The governing equations are determined by Fourier's law of heat conduction:

$$\frac{\partial T_w}{\partial t} = \alpha_w \frac{\partial^2 T_w}{\partial x^2} \qquad 0 < x < X_1 \tag{1}$$

$$\frac{\partial T_I}{\partial t} = \alpha_I \frac{\partial^2 T_I}{\partial x^2} \qquad X_1 < x < X_2 \tag{2}$$

The boundary conditions for the system are:

at x = 0, $T = T_0 = 4°C$ (3)

at x=X_1, $-k_w \frac{\partial T_w}{\partial x} = -k_I \frac{\partial T_I}{\partial x} + \rho_I \lambda_I \frac{dX_1}{dt}$ (4a)

at x = X_1, $T_I = T_w = T_M = 0°C$ (4b)

at x = X_2, $-k_I \frac{\partial T_I}{\partial x} = \varepsilon_H \rho_H \lambda_H \frac{dX_2}{dt}$ (5a)

at x = X_2, $T_I = T_H = T_D$ (5b)

Boundary conditions (3), (4b) and (5b) are due to constant temperatures at the pipe wall, the ice-water interface, and the ice-hydrate interface, respectively. At the ice-water boundary, condition (4a) indicates that heat conduction through the water layer is equal to heat conducted into ice, as well as heat to melt the ice. At the ice-hydrate boundary, condition (5a) equates heat conducted through the ice to the heat to dissociate the hydrate.

2.1b Solution to Model with T_D<273K and Three Phases Present

After solving the differential equations, the constant temperature boundary conditions were applied to obtain the temperature profiles. The temperature profiles were then differentiated to obtain values for the flux boundary conditions (4a and 5a) so that the positions of X_1 and X_2 with time could be calculated. Applying boundary condition (3 and 4b) we get

$$\frac{T_w - T_0}{T_M - T_0} = \frac{erf\,\dfrac{x}{\sqrt{4\alpha_w t}}}{erf\,\xi_1} \tag{6}$$

After applying boundary conditions (4b) and (5b) we get

$$\frac{T_I - T_M}{T_D - T_M} = \frac{erf\,\dfrac{x}{\sqrt{4\alpha_I t}} - erf\left(\xi_1\sqrt{\dfrac{\alpha_w}{\alpha_I}}\right)}{erf\,\xi_2 - erf\left(\xi_1\sqrt{\dfrac{\alpha_w}{\alpha_I}}\right)} \tag{7}$$

where

$$\frac{X_1}{\sqrt{4\alpha_w t}} = \xi_1 \;\; and \;\; \frac{X_2}{\sqrt{4\alpha_I t}} = \xi_2 \tag{8}$$

Equations (6), (7) and (8) may be differentiated and substituted into the boundary conditions given by equations (4a) and (5a) to obtain the following transcendental equations.

$$\frac{e^{-\xi_1^2}}{erf\,\xi_1} = T_D^*\sqrt{\alpha^*}\left[\frac{e^{-\xi_1^2\alpha^*}}{erf\,\xi_2 - erf\left(\xi_1\sqrt{\alpha^*}\right)}\right] + \sqrt{\pi}\,\rho_I^*\,\lambda_I^*\,\xi_1 \tag{9}$$

$$\frac{e^{-\xi_2^2}}{erf\,\xi_2 - erf\left(\xi_1\sqrt{\alpha^*}\right)} = \varepsilon_H\sqrt{\pi}\,\rho_H^*\,\lambda_H^*\,\xi_2 \tag{10}$$

where the dimensionless parameters are defined as follows

$$T^* = \frac{k_I}{k_w}\frac{(T_M - T_D)}{(T_0 - T_M)}, \quad \alpha^* = \frac{\alpha_w}{\alpha_I}, \quad \rho_I^* = \frac{\rho_I}{\rho_W}$$

$$\rho_H^* = \frac{\rho_H}{\rho_I}, \quad \lambda_I^* = \frac{\lambda_I}{C_{p_w}(T_0 - T_M)}, \quad \lambda_H^* = \frac{\lambda_H}{C_{p_I}(T_M - T_D)}$$

The method to solve the model equations was (1) solve the transcendental equations (9 and 10) for the parameters ξ_1 and ξ_2 at the dissociation pressures of interest, then (2) use ξ_1 and ξ_2 in equations (8) to determine movement of the water-ice (X_1) front and the ice-hydrate (X_2) front with time.

Figure 3 shows the progress of the ice-hydrate boundary with time at various temperatures for dissociation of a hydrate layer 15.2 cm thick (the equivalent of radial dissociation in a 0.61m I.D. pipeline). The figure and Table 1 illustrate that hydrate rapidly converts to ice, most readily (about five hours) for the case of -80°C, the temperature corresponding to the case of pipeline depressurization to atmospheric pressure. Other temperatures shown are (-35°C) the Joule-Thomson cooling temperature in the plug when the pipeline is depressured to one atmosphere, and arbitrary temperatures of -10°C and -1.5^{o}C.

Yet in contrast to the ice-hydrate result, the water-ice front is of principal interest, because only at ice removal will the pipeline be free of obstruction. The general solution shows that the conversion of the ice to water is small (always less than 1cm) during the period that 15.2 cm of hydrate is dissociated to ice. When the hydrate phase is depleted in the pipeline, the solution must go from the above three phase solution, to the below two phase solution.

2.1.c. Model at T_D<273K with only Water and Ice Present.

At pipeline pressure reductions such that the hydrate dissociation temperature is less than 273K, when the hydrate phase converts to ice, the ice phase continues to melt due to heat input from the surrounding pipeline at 4°C. The ice conversion to water is regulated by the simpler model shown in Figure 4 when only water and ice are present. The melting of ice is given by the below equations:

$$\frac{\partial T_w}{\partial t} = \alpha_w \frac{\partial^2 T_w}{\partial x^2} \qquad 0 < x < X_1 \tag{11}$$

$$\frac{\partial T_I}{\partial t} = \alpha_I \frac{\partial^2 T_I}{\partial x^2} \qquad X_1 < x < \infty \tag{12}$$

The boundary conditions for the system are:

at $x = 0$, $T = T_0 = 4°C$ (13)

at $x=X_1$, $-k_w \frac{\partial T_w}{\partial x} = -k_I \frac{\partial T_I}{\partial x} + \rho_I \lambda_I \frac{dX_1}{dt}$ (14a)

at $x = X_1$, $T_I = T_w = T_M = 0°C$ (14b)

at $x = \infty$, $T_I = T_D$ (15)

2.1.d Solution to Model with T_D<273K With Only Water and Ice Present

The solution is obtained in a similar manner to the previous case, with the temperature profile in the water phase as:

$$\frac{T_w - T_0}{T_M - T_0} = \frac{erf \frac{x}{\sqrt{4\alpha_w t}}}{erf\, \xi_1} \tag{16}$$

while the temperature profile in the ice phase is given by:

$$\frac{T_I - T_D}{T_M - T_D} = \frac{erfc \frac{x}{\sqrt{4\alpha_I t}}}{erfc\left(\xi_1 \sqrt{\frac{\alpha_w}{\alpha_I}}\right)} \tag{17}$$

Equations (16) and (17) may be differentiated and substituted into the boundary condition given by equation (14a) to obtain the below transcendental equation to be solved for ξ_1

$$\frac{e^{-\xi_1^2}}{erf\, \xi_1} = T_D^* \sqrt{\alpha^*}\left(\frac{e^{-\xi_1^2 \alpha^*}}{erfc\left(\xi_1 \sqrt{\alpha^*}\right)}\right) + \sqrt{\pi}\, \rho_I^* \lambda_I^* \xi_1 \tag{18}$$

so that the position of the moving water-ice boundary X_1 may be plotted as

$$X_1 = \xi_1 \sqrt{4\alpha_w t} \tag{19}$$

Table 2 indicates the time at which the water-ice front has progressed through the slab, corresponding to the center of a pipeline at equivalent pressures and temperature to those shown in Table 1 and the accompanying discussion.

2.1.e. Model at T_D>273K with only Water and Hydrate Present.

If the pipeline dissociation pressure is kept above 2.7 MPa, the dissociation temperature will always be above 273K eliminating the possibility of the ice phase discussed in Sections 2.1.a through 2.1.d. As in Figure 2, the hydrate porosity is such that the hydrate temperature is everywhere the same as determined by the dissociation pressure in the pipeline. In this case the model has only one moving boundary as shown schematically in Figure 5.

The governing equation is

$$\frac{\partial T_w}{\partial t} = \alpha_w \frac{\partial^2 T_w}{\partial x^2} \qquad 0 < x < X(t), t > 0 \tag{20}$$

and the boundary conditions are:

$$\text{at } x = 0, \quad T_w = T_0 \tag{21}$$

$$\text{at } x = X, \quad -k_w \frac{\partial T_w}{\partial x} = \rho_H \lambda_H \frac{dX}{dt} \tag{22a}$$

$$\text{at } x = X, \quad T_w = T_H = 0.3°C \tag{22b}$$

Equation (22b) indicates that the hydrate temperature will always be at 0.3°C.

2.1.f Solution to Model with T_D>273K With Only Water and Hydrate Present

As before, substitution of the temperature boundary conditions, gives the temperature profile as

$$\frac{T_w - T_0}{T_M - T_0} = \frac{erf\,\dfrac{x}{\sqrt{4\alpha_w t}}}{erf\,\lambda} \tag{23}$$

and differentiation of the temperature profile gives the transcendental equation from boundary condition (22a)

$$\frac{e^{-\lambda_1^2}}{erf\,\lambda} = \sqrt{\pi}\,\rho_I^* \lambda_I^* \lambda_1 \tag{24}$$

where the water-hydrate boundary is given with as a function of time by the relation

$$X = \lambda \sqrt{4\alpha_w t} \tag{25}$$

As before, transcendental equation (24) is solved for ξ and then the moving water-hydrate boundary may be determined as a function of time.

Figure 6 contains a line with circles indicating that 15.2cm of hydrate is dissociated in about 425 hours (17.7 days) when the pipeline pressure is kept at 2.4 MPa so that the hydrate dissociation temperature is 0.3^{o}C and ice is never formed.

3. DISCUSSION OF RESULTS

Figure 6 also shows the progress of the ice-hydrate front at -10°C, and the water-ice front at -10°C as the 15.2 cm solid is dissociated. The dashed line indicates that hydrate converts to ice very rapidly (32 hours) compared to either of the other two dissociation line. For the conversion of ice to water (solid line) the change in slope occurs at 32 hours, with the hydrate layer depletion so that the three phase (L_W-I-H) solution (Sections 2.1.a,b) converts to the two-phase (L_W-I) solution (Sections 2.1.c,d). The ice layer is depleted in about 137 hours (5.7 days).

Initially the results of Figure 6 may seem counter-intuitive, when considering the depletion of all solids in the 15.2 cm slab. It is startling that the water-ice layer resulting from hydrate dissociation is depleted faster (5.7 vs. 17.7 days) than the conversion of hydrate to water without an ice intermediate layer. This fact may be reconciled by the realization that two factors promote rapid dissociation when an ice layer is present:

1. the thermal diffusivity ($k/\rho C_p$) of ice is an order of magnitude higher than that of water due to ice's high thermal conductivity and low heat capacity, and
2. the thermal gradient (dT/dx - which controls the heat flux) in the water-hydrate system (without an ice intermediate) is limited to a gradient between the wall temperature (4°C) and 0°C. When ice is present the thermal gradient throughout the ice phase can be much higher, resulting in a higher heat flux.

Figure 7 shows the time calculated for dissociation of all solids (ice and hydrate) from a 15.2cm slab as a function of the hydrate dissociation temperature. The minimum dissociation time occurs at about -15°C, for which the pipeline dissociation pressure is 1.6 MPa. This result is only a function of the pipeline diameter, and is neither a function of the normal pipeline operating pressure nor the length of the plug formed.

It should be stressed that this preliminary work has several limitations:

1. The model should be confirmed via laboratory or field data.
2. The model should be converted to cylindrical dimensions of a pipeline.
3. The most conservative boundary conditions used here, might be modified for more realistic operation. This would make the dissociation time shorter, but the relative times and minimum temperature is not anticipated to change significantly.
4. This model has discounted longitudinal dissociation, assuming that radial dissociation will prevail. Such an assumption could be checked via generation of a similar model which includes an energy balance.

4. CONCLUSION

Several conclusions can be obtained from this preliminary model:

1. Rapidly lowering a pipeline pressure to atmospheric pressure on each side of a hydrate plug may result in rapid conversion of the hydrate plug to an ice plug.

2. At depressurization to a very low pressure, (e.g. atmospheric) the ice plug may require substantially longer to melt than the hydrate plug.

3. The most rapid solution may be obtained by lowering the pipeline pressure to an optimal 1.6 MPa, the point at which hydrates form enough ice to promote a heat flux due to ice's high thermal diffusivity and the high thermal gradient.

5. REFERENCES

1. Sloan, E.D., Clathrate Hydrates of Natural Gases, Chapter 2, Marcel Dekker, Inc., New York (1990)

2. Sloan, E.D., The State-of-the-Art of Hydrates as Related to the Natural Gas Industry, GRI Topical Report, GRI-91/0302 (1992)

3. Lederhos, J.P., Long, J.P., Sum, A. Christiansen, R.L., Sloan, E.D., Chem. Eng. Sci., **51**, 1221, (1996)

4. Reference 1, pp. 491-498

5. Borthne, G. Berge, L., Austvik, R., Gjertsen, L., "Gas Flow Cooling Effect in Hydrate Plug Experiments," Proced. Second Int. Conf. on Natural Gas Hydrates, page 381, June 2-6, 1996, Toulouse, France

6. Lysne, D., An Experimental Study of Hydrate Plug Dissociation by Pressure Reduction, D.Ing.Thesis, Universitetet I Trondheim, Norges, Tekniske Hogskole, pp 7-9 (1995)

7. Reference 1, pp. 455-464

8. Berge, L., Gjertsen, L., Lysne, D., "The Importance of Porosity and Permeability for Dissociation of Hydrate Plugs in Pipes," Proced. Second Int. Conf. on Natural Gas Hydrates, page 533, June 2-6, 1996, Toulouse, France

9. Austvik, T., Husvedt, E., Meland, B., Berge, L.I., Lysne, D., "Tommeliten Gamma Field Hydrate Experiments," Proc. 7th Int. Conf. on Multiphase Production, June 7-9, 1995, Cannes, France, BHR Group Conference Series, Publication No. 14.

List of Figures

1. Pressure-Temperature Phase Diagram for Methane Hydrates

Figure 2a. Hydrate Dissociation Schematic, with Phases (Progressing inward) of the Pipewall, Water, Ice, and Hydrate

Figure 2b. Qualitative Temperature Profile Through the Wall, Water Layer, Ice Layer, and Hydrate Layer

Figure 3. Movement of the Ice-Hydrate Front as a Function of Temperature (diamonds = -80°C with depressurization to atmospheric conditions, squares =-35°C at maximum Joule-Thomson cooling of hydrate, triangles at -10°C, x's at -1.5^{o}C)

Figure 4. Qualitative Temperature Profile in the Water-Ice Layer After Hydrate Dissociation Below 273K

Figure 5. Qualitative Temperature Profile in the Water-Hydrate Layer as Hydrate is Dissociated Above 273K

Figure 6. Rate of Solid Front Movement with Time to Dissociate a 15.2cm Hydrate Slab. (dotted line = water-hydrate front at -10°C, dashed line = ice-hydrate front, solid line = water-ice front at -10°C with change in slope after hydrate dissociation as three phase (L_W-I-H) solution becomes a two phase (L_W-I) solution below 0°C)

Figure 7. Time to Dissociate 15.2 cm of Hydrate as a Function of Dissociation Temperature.

List of Tables;

Table 1. Conversion of 15.2cm of Hydrate to Ice as a Function of Dissociation Pressure

Table 2. Time to Convert 15.2 cm of Ice to Water as a Function of Dissociation Pressure

Table 1: Conversion of 15.2cm of Hydrate to Ice as a Function of Dissociation Pressure

Hydrate Temperature, °C	-80	-35	-10	-1.5
Corresponding Pressure (MPa)	0.10	0.84	1.8	2.6
Time (Hours) to convert 15.2 cm of hydrate to ice	5	10	32	156

Table 2: Time to Convert 15.2 cm of Ice to Water as a Function of Dissociation Pressure

Hydrate Temperature, °C	-80	-35	-10	-1.5
Corresponding Pressure (MPa)	0.10	0.84	1.8	2.6
Time (Hours) to convert 15.2 cm of ice to water	2049	486	137	188

Figure 1

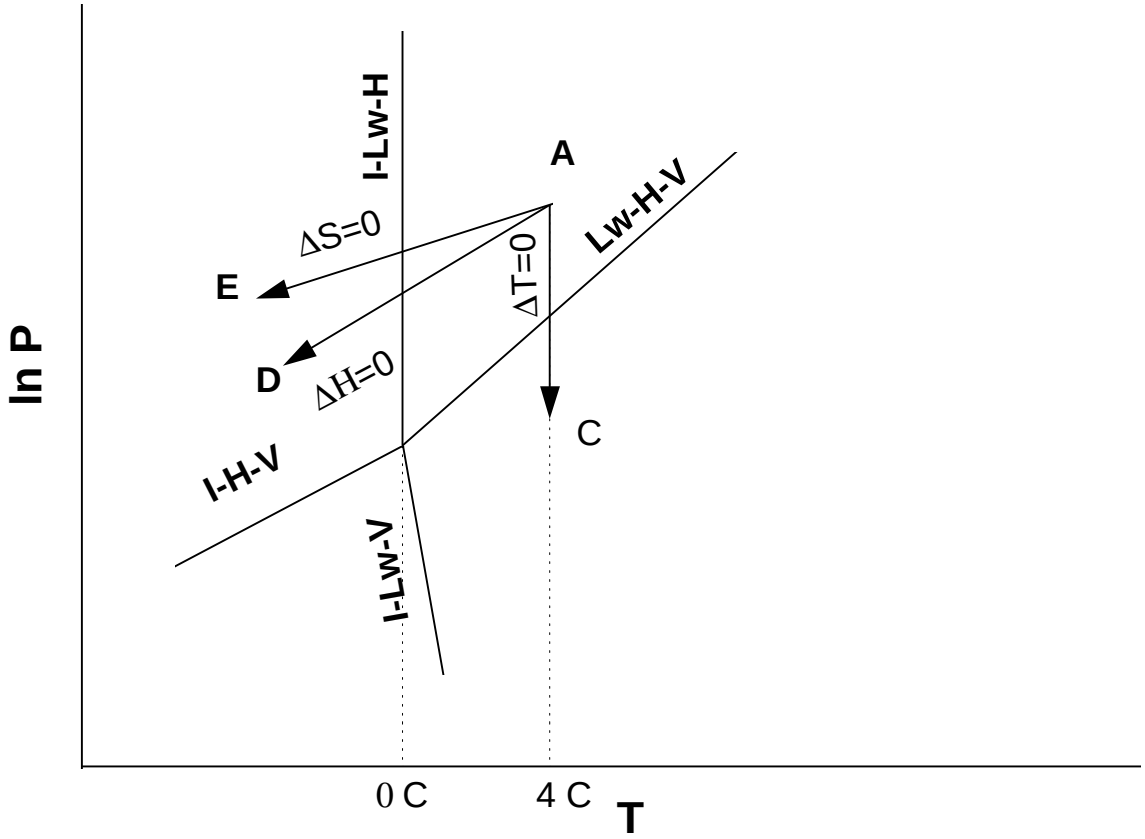

Figure 2a and 2b

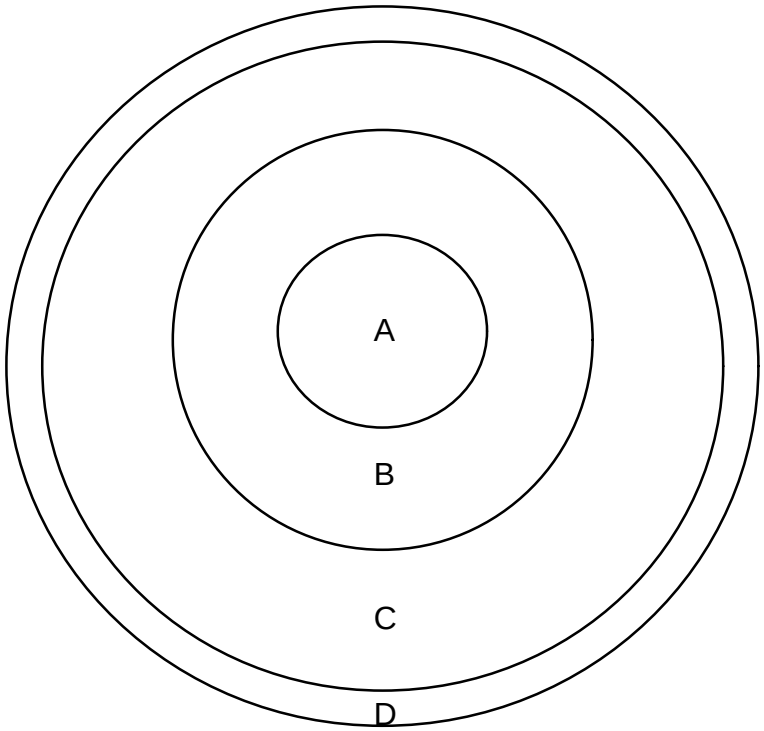

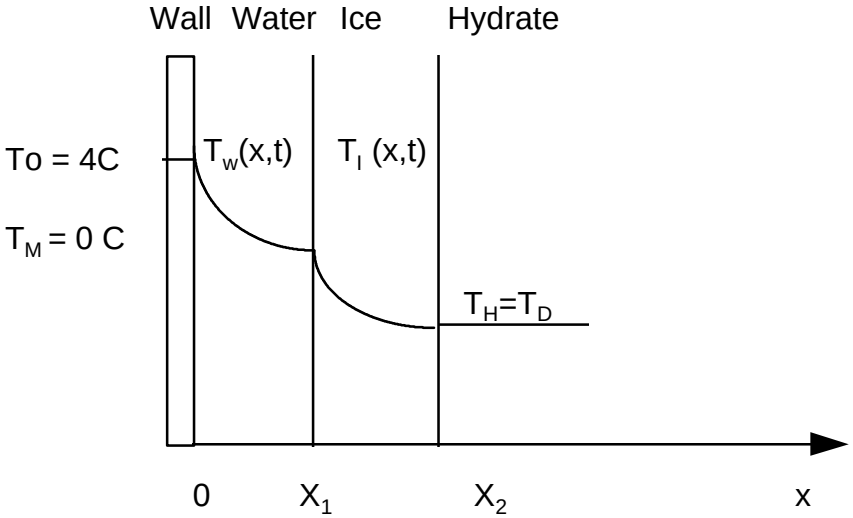

Figure 3

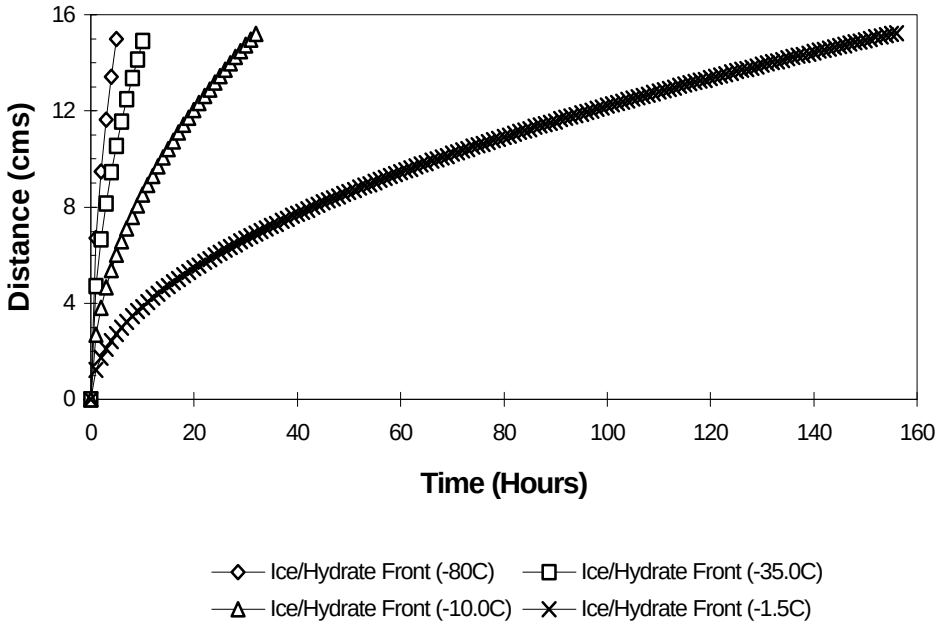
16
12
8
4
0
Distance (cms)
0
20
40
60
80
100
120
140
160
Time (Hours)
Ice/Hydrate Front (-80C)
Ice/Hydrate Front (-35.0C)
Ice/Hydrate Front (-10.0C)
Ice/Hydrate Front (-1.5C)

Figure 4

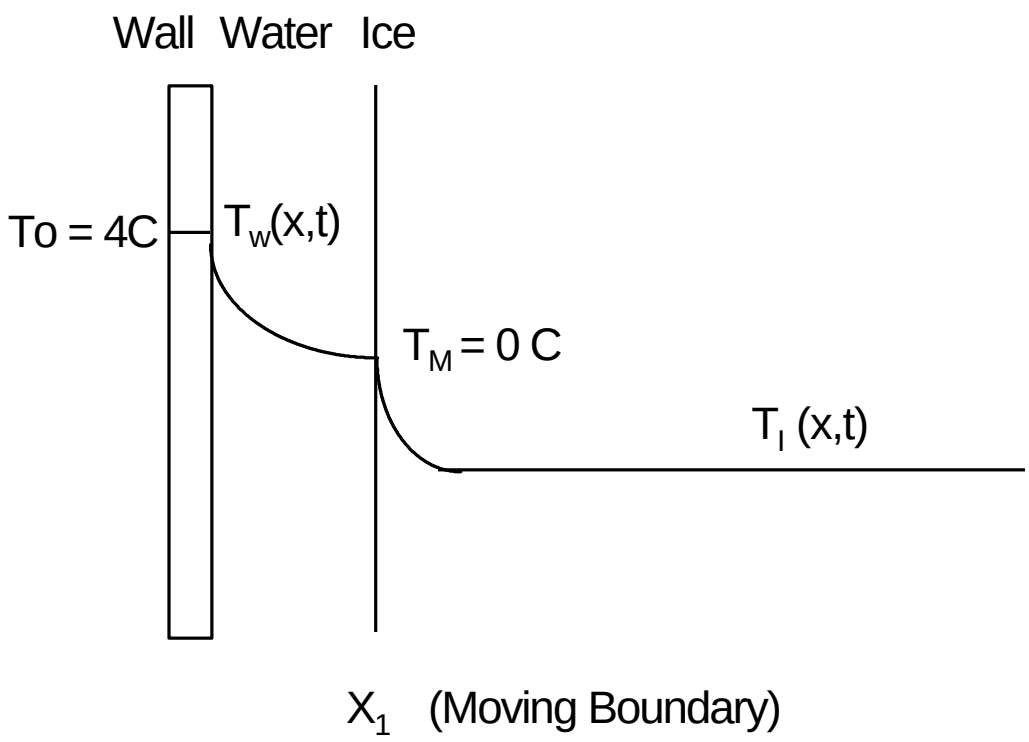

Figure 5

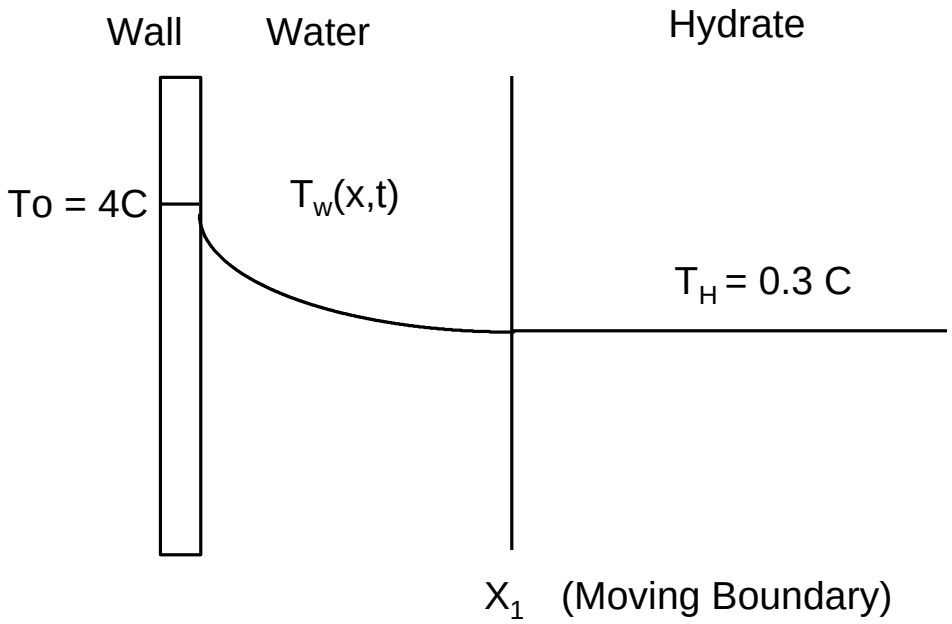

Figure 6

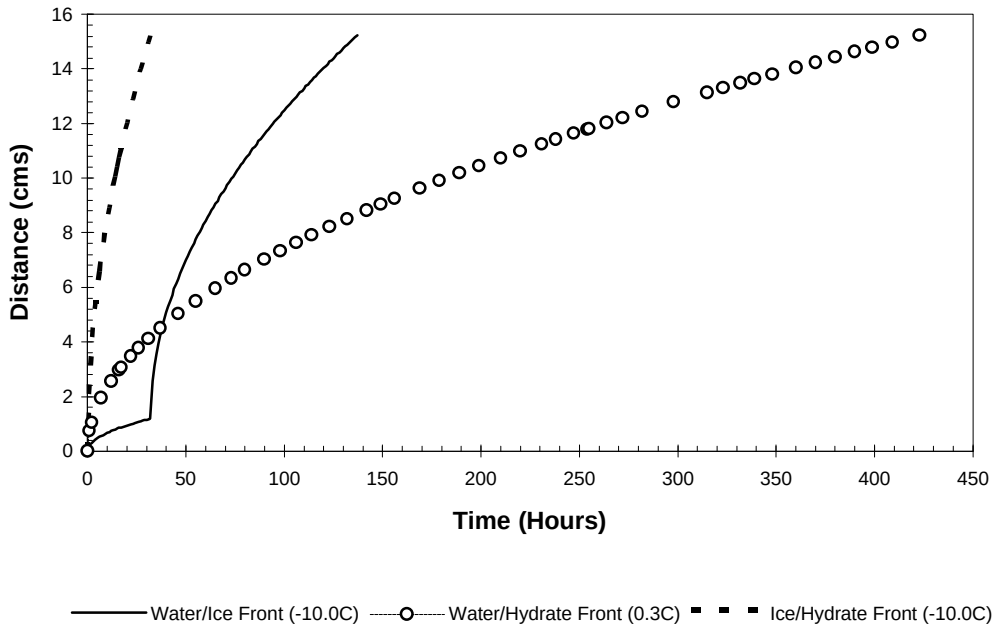
Distance (cms)
Time (Hours)
0
2
4
6
8
10
12
14
16
0
50
100
150
200
250
300
350
400
450
Water/Ice Front (-10.0C)
Water/Hydrate Front (0.3C)
Ice/Hydrate Front (-10.0C)

Figure 7

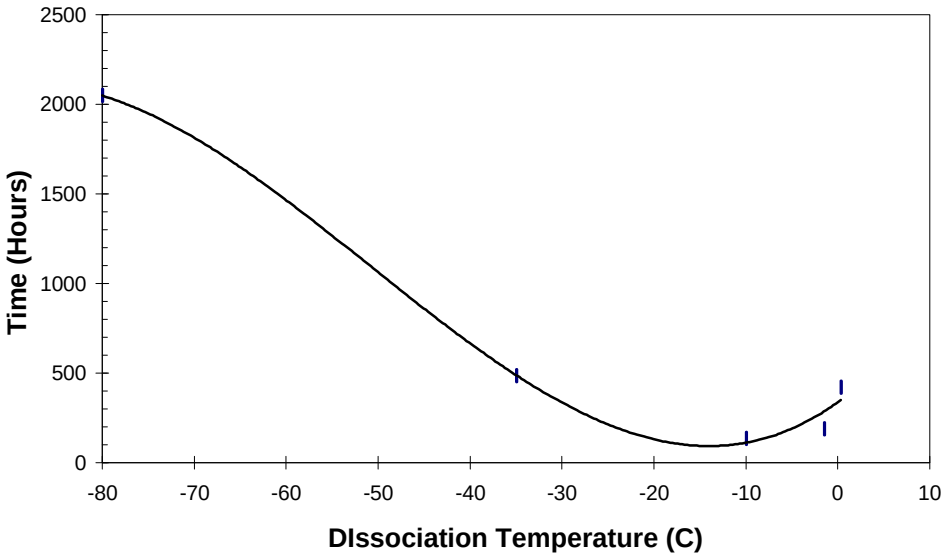
2500
2000
1500
1000
500
0
Time (Hours)
-80
-70
-60
-50
-40
-30
-20
-10
0
10
DIssociation Temperature (C)